Observation of strong cascaded Kerr-lens dynamics in an optimally-coupled cw intracavity frequency-doubled Nd:YLF ring laser

Jean-Jacques Zondy,[1]* Fabiola A. Camargo,[1,2] Thomas Zanon,[1] Valentin Petrov,[3] and Niklaus U. Wetter[2]

[1]*Laboratoire Commun de Métrologie LNE-Cnam, 61 rue du Landy, F-93210 La Plaine Saint Denis, France*
[2]*Instituto de Pesquisas Energéticas e Nucleares (CNEN-IPEN/SP), CEP 005508-000 São Paulo, Brazil*
[3]*Max-Bom-Institute for Nonlinear Optics and Ultrafast Spectroscopy, 2A Max-Bom-Str., D-12489 Berlin, Germany*
**jean-jacques.zondy@cnam.fr*

Abstract: Self-starting self-pulsing dynamics at the cavity free-spectral-range frequency were observed in intracavity second-harmonic generation of a diode end-pumped Nd:YLF ring laser containing a periodically-poled $KTiOPO_4$ (ppKTP) nonlinear crystal. Although the unidirectional laser was designed for continuous-wave (cw) single-frequency operation, with a resonator set at the middle of its stability range, partial Kerr-lens mode-locking (KLM) arose spontaneously once the ppKTP was inserted. This ultrafast dynamics along with a strong spectral gain broadening, not observed with any birefringent nonlinear doubler, is associated to the finite bandwidth of the quasi-phase-matched crystal with respect to the laser gain bandwidth, leading to giant cascaded Kerr-lensing effects when the ppKTP temperature is detuned from perfect quasi-phase-matching either in the self-focusing or defocusing sides. While under partial KLM operation the laser delivered only ~0.14W of broadband red output power, single-frequency operation could be only achieved by using an intracavity etalon with a suitable partial reflectivity (R≥25%), leading to an optimally (~100% efficiency) out-coupled 1.4W red power at 660.5nm, as much as the fundamental 1321nm power that could be extracted from the unidirectional laser using an optimal $T = 2\%$ output coupler.

OCIS codes: (190.4410) Nonlinear optics, parametric processes; (190.3100) Instabilities and chaos; (190.3270) Kerr effects; (140.3560) Lasers, ring; (140.3515) Lasers, frequency doubled; (140.3515) Lasers, single-mode; (140.4050) Mode-locked lasers.

References and links

1. H. Ogilvy, M. J. Withford, P. Dekker, and J. A. Piper, "Efficient diode double-end-pumped Nd:YVO4 laser operating at 1342nm," Opt. Express **11**(19), 2411–2415 (2003).
2. Y. Inoue, S. Konno, T. Kojima, and S. Fujikawa, "High-power red beam generation by frequency-doubling of a Nd:YAG Laser," IEEE J. Quantum Electron. **35**(11), 1737–1740 (1999).
3. A. Agnesi, A. Guandalini, G. Reali, S. Dell'Acqua, and G. Piccinno, "High-brightness 2.4-W continuous-wave Nd:$GdVO_4$ laser at 670 nm," Opt. Lett. **29**(1), 56–58 (2004).
4. A.-Y. Yao, W. Hou, Y. Bi, A.-C. Geng, X.-C. Lin, Y.-P. Kong, D.-F. Cui, L.-A. Wu, and Z.-Y. Xu, "High-power cw 671 nm output by intracavity frequency doubling of a double-end-pumped Nd:YVO_4 laser," Appl. Opt. **44**(33), 7156–7160 (2005).
5. H. Y. Zhu, G. Zhang, C. H. Huang, Y. Wei, L. X. Huang, and Z. Q. Chen, "8.1 W/670.7 nm and 5.1 W/669.6 nm cw red light outputs by intracavity frequency doubling of a Nd:YAP laser with LBO," Appl. Phys. B **91**(3-4), 433–436 (2008).
6. Y. Louyer, P. Juncar, M. D. Plimmer, T. Badr, F. Balembois, P. Georges, and M. E. Himbert, "Doubled single-frequency Nd:YLF ring laser coupled to a passive nonresonant cavity," J. Opt. Soc. Am. B **43**, 1773–1776 (2004).
7. R. Sarrouf, V. Sousa, T. Badr, G. Xu, and J.-J. Zondy, "Watt-level single-frequency tunable Nd:YLF/periodically poled $KTiOPO_{(4)}$ red laser," Opt. Lett. **32**(18), 2732–2734 (2007).
8. R. Sarrouf, T. Badr, and J.-J. Zondy, "Intracavity second-harmonic generation of diode-pumped continuous-wave, single-frequency 1.3μm Nd:$YLiF_4$ lasers," J. Opt. A, Pure Appl. Opt. **10**(10), 104011 (2008).

#121572 - $15.00 USD Received 17 Dec 2009; revised 28 Jan 2010; accepted 29 Jan 2010; published 23 Feb 2010

9. F. A. Camargo, T. Zanon-Willette, T. Badr, N. U. Wetter, and J.-J. Zondy, "Tunable single-frequency Nd:YVO_4 /BiB_3O_6 ring laser at 671nm," IEEE J. Quantum Electron. (to be published).
10. A. Agnesi, G. C. Reali, and P. G. Gobbi, "430-mW single-transverse-mode diode-pumped Nd:YVO_4 laser at 671 nm," IEEE J. Quantum Electron. **34**(7), 1297–1300 (1998).
11. K. I. Martin, W. A. Clarkson, and D. C. Hanna, "3 W of single-frequency output at 532 nm by intracavity frequency doubling of a diode-bar-pumped Nd:YAG ring laser," Opt. Lett. **21**(12), 875–877 (1996).
12. Y. Zheng, H. Lu, F. Li, K. Zhang, and K. Peng, "Four watt long-term stable intracavity frequency-doubling Nd:YVO_4) laser of single-frequency operation pumped by a fiber-coupled laser diode," Appl. Opt. **46**(22), 5336–5339 (2007).
13. R. Polloni, and O. Svelto, "Optimum coupling for intracavity second harmonic generation," IEEE J. Quantum Electron. **4**(9), 528–530 (1968).
14. R. G. Smith, "Theory of intracavity optical second-harmonic generation," IEEE J. Quantum Electron. **6**(4), 215–223 (1970).
15. G. Cerullo, S. De Silvestri, A. Monguzzi, D. Segala, and V. Magni, "Self-starting mode locking of a cw Nd:YAG laser using cascaded second-order nonlinearities," Opt. Lett. **20**(7), 746–748 (1995).
16. M. Zavelani-Rossi, G. Cerullo, and V. Magni, "Mode-locking by cascading of second-order nonlinearities," IEEE J. Quantum Electron. **34**(1), 61–70 (1998).
17. K. A. Stankov, and J. Jethwa, "A new mode-locking technique using a nonlinear mirror," Opt. Commun. **66**(1), 41–46 (1988).
18. K. A. Stankov, "Mode locking by a frequency-doubling crystal: generation of transform-limited ultrashort light pulses," Opt. Lett. **14**(7), 359–361 (1989).
19. M. B. Danailov, G. Cerullo, V. Magni, D. Segala, and S. De Silvestri, "Nonlinear mirror mode locking of a cw Nd:YLF laser," Opt. Lett. **19**(11), 792–794 (1994).
20. Y. F. Chen, S. W. Tsai, and S. C. Wang, "High-power diode-pumped nonlinear mirror mode-locked Nd:YVO_4," Appl. Phys. B **72**, 395–397 (2001).
21. S. J. Holmgren, V. Pasiskevicius, and F. Laurell, "Generation of 2.8 ps pulses by mode-locking a Nd:$GdVO_4$ laser with defocusing cascaded Kerr lensing in periodically poled KTP," Opt. Express **13**(14), 5270–5278 (2005).
22. R. DeSalvo, D. J. Hagan, M. Sheik-Bahae, G. Stegeman, E. W. Van Stryland, and H. Vanherzeele, "Self-focusing and self-defocusing by cascaded second-order effects in KTP," Opt. Lett. **17**(1), 28–30 (1992).
23. G. I. Stegeman, M. Sheik-Bahae, E. Van Stryland, and G. Assanto, "Large nonlinear phase shifts in second-order nonlinear-optical processes," Opt. Lett. **18**(1), 13–15 (1993).
24. D. E. Spence, P. N. Kean, and W. Sibbett, "60-fsec pulse generation from a self-mode-locked Ti:sapphire laser," Opt. Lett. **16**(1), 42–44 (1991).
25. T. Brabec, Ch. Spielmann, P. F. Curley, and F. Krausz, "Kerr lens mode locking," Opt. Lett. **17**(18), 1292–1294 (1992).
26. G. P. A. Malcolm, and A. I. Ferguson, "Self-mode locking of a diode-pumped Nd:YLF laser," Opt. Lett. **16**(24), 1967–1969 (1991).
27. G. Cerullo, S. D. Silvestri, and V. Magni, "Self-starting Kerr-lens mode locking of a Ti:sapphire laser," Opt. Lett. **19**(14), 1040–1042 (1994).
28. J. R. Lincoln, and A. I. Ferguson, "All-solid-state self-mode locking of a Nd:YLF laser," Opt. Lett. **19**(24), 2119–2121 (1994).
29. K. Tamura, J. Jacobson, E. P. Ippen, H. A. Haus, and J. G. Fujimoto, "Unidirectional ring resonators for self-starting passively mode-locked lasers," Opt. Lett. **18**(3), 220–222 (1993).
30. W. S. Pelouch, P. E. Powers, and C. L. Tang, "Self-starting mode-locked ring-cavity Ti:sapphire laser," Opt. Lett. **17**(22), 1581–1583 (1992).
31. A. Agnesi, "Kerr-lens modelocking of solid-state lasers and unidirectional cavities," IEEE J. Quantum Electron. **30**(4), 1115–1121 (1994).
32. D. R. Heatley, A. M. Dunlop, and W. J. Firth, "Kerr lens effects in a ring resonator with an aperture: mode locking and unidirectional operation," Opt. Lett. **18**(2), 170–172 (1993).
33. S. Greenstein, and M. Rosenbluh, "The influence of nonlinear spectral bandwidth on single longitudinal mode intra-cavity second harmonic generation," Opt. Commun. **248**(1-3), 241–248 (2005).
34. S. Greenstein, and M. Rosenbluh, "Dynamics of cw intra-cavity second-harmonic generation by PPKTP," Opt. Commun. **238**(4-6), 319–327 (2004).
35. M. Pierrou, F. Laurell, H. Karlsson, T. Kellner, C. Czeranowsky, and G. Huber, "Generation of 740 mW of blue light by intracavity frequency doubling with a first-order quasi-phase-matched KTiOPO($_4$) crystal," Opt. Lett. **24**(4), 205–207 (1999).
36. T. Baer, "Large-amplitude fluctuations due to longitudinal mode coupling in diode-pumped intracavity-doubled Nd:YAG lasers," J. Opt. Soc. Am. B **3**(9), 1175–1180 (1986).
37. A. Sennaroglu, "Broadly tunable continuous-wave orange-red source based on intracavity-doubled Cr^{4+}:forsterite laser," Appl. Opt. **41**(21), 4356–4359 (2002).
38. R. Fluck, G. Zhang, U. Keller, K. J. Weingarten, and M. Moser, "Diode-pumped passively mode-locked 1.3-microm Nd:YVO(4) and Nd:YLF lasers by use of semiconductor saturable absorbers," Opt. Lett. **21**(17), 1378–1380 (1996).
39. H. D. Sun, G. J. Valentine, R. Macaluso, S. Calvez, D. Burns, M. D. Dawson, T. Jouhti, and M. Pessa, "Low-loss 1.3-μm GaInNAs saturable Bragg reflector for high-power picosecond neodymium lasers," Opt. Lett. **27**(23), 2124–2126 (2002).

#121572 - $15.00 USD Received 17 Dec 2009; revised 28 Jan 2010; accepted 29 Jan 2010; published 23 Feb 2010

40. V. Liverini, S. Schön, R. Grange, M. Haiml, S. C. Zeller and U. Keller, "A low-loss GaInNAs SESAM mode-locking a 1.3-μm", paper CThV7, CLEO 2004 Technical Digest (OSA).
41. P. J. Hardman, W. A. Clarkson, G. J. Friel, M. Pollnau, and D. C. Hanna, "Energy-Transfer upconversion and thermal lensing in high-power end-pumped Nd: YLF laser crystals," IEEE J. Quantum Electron. **35**(4), 647–655 (1999).
42. K. Fradkin, A. Arie, A. Skliar, and G. Rosenman, "Tunable midinfrared source by difference frequency generation in bulk," Appl. Phys. Lett. **74**(7), 914–916 (1999).
43. J.-J. Zondy, "Comparative theory of walkoff-limited type-II versus type-I second-harmonic generation with Gaussian beams," Opt. Commun. **81**(6), 427–440 (1991).
44. K. I. Martin, W. A. Clarkson, and D. C. Hanna, "Self-suppression of axial mode hopping by intracavity second-harmonic generation," Opt. Lett. **22**(6), 375–377 (1997).
45. P. De Natale, I. Galli, G. Giusfredi, D. Mazzotti, and P. Cancio, "Functional periodically-poled crystals for powerful intracavity CW difference-frequency-generation of widely tunable, high spectral purity IR radiation," Proc. SPIE **7031**, 70310K (2008).
46. C. Sibilia, A. Re, E. Fazio, and M. Bertolotti, "Cascading effect on second-harmonic generation in a ring cavity," J. Opt. Soc. Am. B **13**(6), 1151–1159 (1996).
47. P.-A. Belanger, and C. Pare, "Self-focusing of Gaussian beams: an alternate derivation," Appl. Opt. **22**(9), 1293–1295 (1983).
48. J.-J. Zondy, D. Touahri, and O. Acef, "Absolute value of the d_{36} nonlinear coefficient of $AgGaS_2$: prospect for a low-threshold doubly-resonant oscillator-based 3:1 frequency divider," J. Opt. Soc. Am. B **14**(10), 2481–2497 (1997).

1. Introduction

Watt-level single-frequency and tunable solid-state lasers are interesting compact alternative to broadly tunable but costly and maintenance-demanding dye-lasers for high-resolution atomic spectroscopy in the visible range. While continuous-wave (cw) intracavity second-harmonic generation (ICSHG) of diode-pumped 1.3μm ($^4F_{3/2}$-$^4I_{13/2}$) Nd-lasers has been widely addressed in the literature in terms of (multimode) power scaling [1–5], very few works have dealt with single-frequency (*i.e.* single longitudinal mode or SLM) and tunable operation for which watt-level red power is still a challenge due to the much weaker 1.3μm emission cross-sections and to unavoidable extra-loss brought by intracavity elements such as a Faraday optical diode and a thin etalon [6–9]. The largest SLM red power (~0.9W) was achieved with a σ-polarized Nd:YLF/ppKTP laser at 657nm [7]. Agnesi *et al* have reported SLM operation of a Nd:YVO_4/LBO laser at 671nm using a standing-wave cavity in which the type-II cut LBO crystal acted as a birefringent filter, but due to hole-burning effects the maximum SLM power was limited to operation near the threshold, yielding 0.37W of red power [10]. This SLM power has been recently increased to 0.68W using a unidirectional ring resonator [9]. Single-frequency diode-pumped solid-state lasers (DPSSLs) have mostly been demonstrated on the much stronger (and narrower, $\Delta\lambda_G$<1nm) ~1μm transitions ($^4F_{3/2}$-$^4I_{11/2}$), yielding multi-watt of green power [11,12]. So far, in all reported cw ICSHG laser performance (SLM or multimode), the overall SH conversion efficiency did not exceed 50% of the optimally available fundamental power that can be extracted from the laser cavity under an optimal output coupler. Even high power cw commercial green lasers delivering more than 10W output power are limited in converting more than 50% of the available fundamental power. Actually, according to the theory of optimally-coupled ICSHG laser developed by Polloni *et al* [13] and Smith [14] it is theoretically possible to convert 100% of the optimally available fundamental-wave (FH) power from the laser by tailoring the SHG nonlinearity to the gain medium spectroscopic properties. Shortly speaking, to reach the optimally-coupled regime either an excessively long nonlinear crystal must be used (typically l_c ~10cm for most birefringence phase-matched materials with d_{eff} ≤3pm/V) or a strong focusing is required to increase the ratio w/w_0 of the pump waist at the gain medium to that inside the nonlinear crystal, with unavoidable side effects such as thermal effects or spurious oscillation on weaker adjacent Nd^{3+} emission lines [11].

In this work we demonstrate such a ~100% conversion efficiency in a π-polarized (λ = 1321.5nm) single-frequency Nd:YLF/ppKTP unidirectional ring laser that satisfies the criterion of optimal ICSHG coupling as derived by Polloni *et al* and Smith. At 14W of absorbed diode pump power (λ_p = 806nm), using a l_c = 10mm long ppKTP (d_{eff} = 9pm/V), a l_G = 10mm long Nd:YLF gain medium and a unidirectional ring cavity designed to give w/w_0

#121572 - $15.00 USD Received 17 Dec 2009; revised 28 Jan 2010; accepted 29 Jan 2010; published 23 Feb 2010

~6.5, we could achieve 1.4W of red power, as much as the SLM optimal fundamental power output achieved with a $T = 2\%$ optimal output coupler, realizing hence the theoretical prediction of optimally-coupled ICSHG lasers (Section 4). The use of ppKTP as the intracavity doubler was determining in achieving this performance, since its replacement with a LBO or BiBO led to conversion efficiencies (with respect to the concept of *optimal* SHG coupling) not exceeding 50% of the available FH power.

Furthermore, we also report on the occurrence of an unexpected dynamical regime related to the use of ppKTP in our ring cavity which operates at the middle of its stability range with a stability parameter $\eta = (A + D)/2 \sim 0$, where ABCD is the roundtrip cavity matrix. This dynamical regime, in the form of a sustained but non stationary train of ~250ps pulses at the cavity free-spectral-range ($f_{rep} = 1/FSR_{cav} = 420$ MHz), is attributed to partial Kerr-lens mode-locking (KLM) triggered by complex cascaded second-order nonlinearities mediated by the highly nonlinear material under phase-mismatched SHG. Although passively mode-locked picosecond lasers based on cascaded $\chi^{(2)}$:$\chi^{(2)}$ processes (also called CSM mode-locking) has been experimentally demonstrated for the first time in 1995 [15], all subsequent demonstrations and theoretical analysis [16] were conducted in standing-wave configurations and necessitated a second pass of the forwardly generated SH wave into the intracavity nonlinear crystal, with a proper phase shift of the back-reflected SH. Under total SH reflection by the dichroic cavity end-mirror with partial transmission of the fundamental wave (FH), the mode-locking process (that uses the amplitude modulation of the effective Kerr nonlinearity, *i.e*. the imaginary part of the effective $\chi^{(3)}$ nonlinearity) is often referred to as *nonlinear mirror* mode-locking (NLM) [17–21]. When both the SH and FH waves are totally reflected, the mode-locking process (that uses the $\chi^{(2)}$:$\chi^{(2)}$ cascaded nonlinear phase shift [22,23], i.e. the real part of the effective Kerr nonlinearity) is then referred to as *cascaded second-order* mode-locking (CSM) [15,16]. Both NLM and CSM require that the laser cavity operates close to one of the stability limits of the resonator, eventually necessitating an intracavity hard aperture for the power-dependent loss modulation and a critical positioning of the effective Kerr medium with respect to the beam focus as in $\chi^{(3)}$-based KLM standing-wave [24–28] or ring resonators [29–32]. However to date CSM has only been reported in a standing-wave resonators and relies on full back-conversion of the SH wave into the FH wave during the second pass in the SHG crystal, which is not the case in our ring cavity for which the SHG interaction is of the single-pass kind, excluding thus any nonlinear mirror scenario. Another peculiarity in this experiment originally aimed at achieving a cw optimally-coupled ICSHG laser is that the ring resonator operates at the middle of its stability range ($\eta = 0$), while KLM and CSM lasers require $|\eta| \rightarrow 1$ to boost the small amplitude power-dependent loss modulation. Even though the mode-locking is only partial (in the sense that the pulse contrast is not 100%), it cannot be explained in the frame of the previously developed NLM or CSM theories based on a double-pass SHG. The mechanism leading to the observed dynamics is most probably related instead to pure KLM effects as described in the ring resonator analysis of Agnesi which considers a thin Kerr medium [31]. Experimentally, the cascaded KLM dynamics reported here bears some similarity with the soft-aperture KLM Ti:Sa ring laser containing an optical diode demonstrated by Tamura *et al* or Pelouch *et al*, in which the unidirectional ring resonator was found to favor self-starting mode-locking owing to the absence of spurious etalon effects characterizing standing-wave KLM resonator [29,30]. Another specificity pledging for pure Kerr-lensing effects rather than NLM or CSM scenario (or both) is that these dynamics arises whichever the sign of the cascaded Kerr nonlinearity unlike the limited range of parameters (such as operation of the laser in the thermal roll-over regime and near the resonator stability limit [21]) characterizing CSM.

The fact that this partial mode-locking dynamics was not observed when either a LBO, BBO or BiBO nonlinear crystals are employed finds also probably its origin in the much narrower spectral SHG acceptance bandwidth of the $l_c = 10$mm long ppKTP ($\Delta\lambda_{NL} = 0.9$nm) as compared to the laser transition gain bandwidth ($\Delta\lambda_G \sim 5$nm at 1.32μm in the fluoride host, while $\Delta\lambda_G \leq 1$nm for the 1.05-1.06μm stronger $^4F_{3/2}$-$^4I_{11/2}$ transition). The ratio $\gamma = \Delta\lambda_{NL}/\Delta\lambda_G$ has been indeed recognized to be a critical parameter in the stable single-frequency behaviour

#121572 - $15.00 USD Received 17 Dec 2009; revised 28 Jan 2010; accepted 29 Jan 2010; published 23 Feb 2010

of cw ICSHG lasers [33]. This finite spectral bandwidth of the ppKTP crystal (γ ~0.2) together with the unidirectional ring configuration may explain why this partial mode-locking dynamics was not reported in a previous cw ICSHG of a 1064nm Nd:YAG/ppKTP standing-wave laser in which only the impact of bistable dynamics induced by the ppKTP on the oscillation wavelength were reported, but no ultrafast temporal dynamics [34]. Similarly, in a 946nm ($^4F_{3/2} \rightarrow {}^4I_{9/2}$) cw ICSHG standing-wave laser employing a thick ppKTP doubler, no Kerr-lens induced dynamics was reported [35], although some observed intensity instabilities in the SH blue output power were attributed to the so-called *green problem* [36], which originates rather from gain cross-coupling of many longitudinal modes via sum-frequency processes and which leads to chaotic (rather than periodic) intensity fluctuations on a time scale of the order or greater than the cavity photon lifetime. As a last example of a cw ICSHG laser employing both a narrow spectral bandwidth pp-material (PPLN) in conjunction with a broad gain bandwidth medium (Cr^{4+}:fosterite), we quote the red-orange tunable (613-655nm) laser achieved by Sennaroglu [37], albeit using again a standing-wave cavity. In this latter work, red power fluctuations as high as ± 60% was reported when the PPLN is strongly temperature detuned from QPM condition, but no characterization of this intensity instability was provided by the author who attributed them to thermal effects in the lasing crystal. While passive self-starting mode-locking of a Nd:YLF laser has been demonstrated only on the stronger 1047nm line using either NLM [19] or KLM (using a glass rod as the $\chi^{(3)}$ medium) [26], passive mode-locking on the weaker 1.32μm transition could be only observed using a semi-conductor saturable absorber (SESAM) [38–40]. This work is the first report to our knowledge of a self-starting (partially) mode-locked Nd:YLF ring laser operating on the broader 1321nm transition without any restriction on the cascaded Kerr nonlinearity sign (positive or negative), and without the requirement of a resonator operating on the verge of its stability range as in [19,26].

This paper is organized as follows. Section 2 starts with the experimental description of the ICSHG laser setup. In section 3 we describe and characterize the temporal and spectral features of the partial mode-locking behavior as function of the ppKTP phase-matching temperature or the pump power. Broad emission spectra ($\Delta\lambda_G$ ~4nm) extending up to the full laser transition bandwidth are observed on the fundamental and SH range, whichever the ppKTP temperature in the range T = 15-70°C (the ppKTP is phase-matched for the 1321.3nm central gain wavelength near T~30°C). In section 4 we analyze the cw single-frequency performance of the optimally-coupled ICSHG laser, when a partially-coated etalon is inserted so as to quench the cascaded second-order processes. Cw single-frequency regime with optimal SH conversion efficiency required a delicate adjustment of the intracavity etalon and ppKTP. But once achieved, a record 1.4W of stable SLM red power at 661nm – as much as the maximum SLM FH power that could be extracted with a T = 2% output coupler – was obtained, reaching for the first time to our knowledge the predicted regime of 100% conversion efficiency characterizing an optimally-coupled cw ICSHG laser [13,14].

2. Experimental ICSHG laser setup

The experimental setup of the cw single-frequency ICSHG ring laser is sketched in Fig. 1. The laser cavity is an asymmetric bow-tie ring cavity consisting of 4 dichroic mirrors (R > 99.9% at 1.32μm with T~90% at 0.66μm and 0.806μm). The radius of curvature of M3 and M4 was ROC = −100mm and the total ring cavity length was L_{cav} = 680mm, with a distance M3-M4 equal to 115mm, M4-M2 = 135mm, M2-M1 = 210mm and M1-M3 = 220mm. From ABCD matrix calculations, the cavity operated at the center of its stability range with respect to the curved mirror spacing (yielding a cavity stability parameter $\eta = (A + D)/2 \approx -5 \times 10^{-2}$ with A = −10.041 and D = + 9.938), with a smaller waist w_0 = 48μm inside the nonlinear crystal (ppKTP) and a larger waist w = 317μm at the center of the Nd:YLF crystal, located ~45mm from M1. The gain-medium to nonlinear-crystal waist ratio was thus w/w_0 ~6.5. Calculations also showed that the larger waist w is very sensitive to a small variation in the M3-M4 spacing, despite the fact the resonator operated at the middle of the stability range:

#121572 - $15.00 USD Received 17 Dec 2009; revised 28 Jan 2010; accepted 29 Jan 2010; published 23 Feb 2010

Increasing (decreasing) this distance by ~1mm leads to a decrease (increase) in w by ~5% while the smaller waist remains almost unaffected. Taking account of the intracavity elements (n_{YLF} = 1.47, n_{ppKTP} = 1.82, n_{TGG} = 1.95), the optical path of the cavity was L_{opt} = 711.9mm, corresponding to a longitudinal mode separation of $FSR_{cav} = c/L_{opt}$ = 421.4MHz.

The laser crystal (an *a*-cut 0.8 at.% doped, 3 × 3 × 10mm^3 Nd:YLF from Crystech Inc.) was longitudinally pumped by a 200μm-core diameter (NA = 0.22) fiber-coupled diode emitting at 806nm that was focused to a w ~265μm waist at the crystal center by a pair of achromatic lenses (f = 80mm and 100mm). The Nd:YLF crystal facets were AR-coated at 1321nm (R<0.5%) and 806nm (R<2%), with a small enough reflectivity (R<20%) at 1050nm to prevent parasitic lasing on the stronger main transition. We have noticed that by removing the ppKTP out of the cavity (in which case η = + 0.356, w_0 = 47μm and w = 255μm, smaller than the pump waist) resulted in a lasing on a TEM_{10} mode rather than a TEM_{00} mode in presence of the ppKTP, highlighting the importance of pump-waist to cavity-waist mode-matching in the presence of the nonlinear crystal.

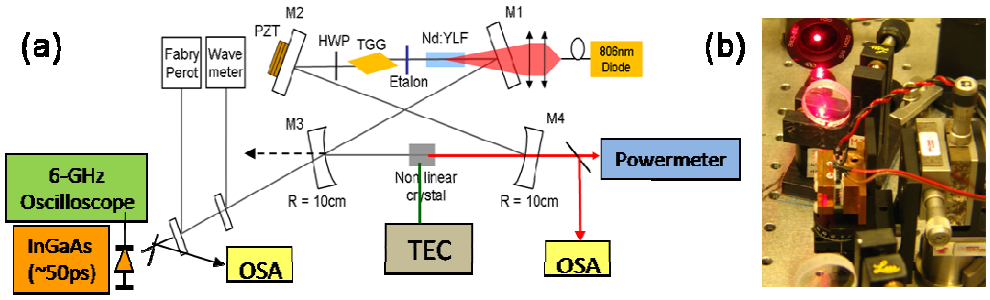

Fig. 1. (a) Experimental ring laser setup. TEC: thermo-electric cooler; OSA: optical spectrum analyzer; (b) Photograph of the ppKTP chip in its TEC-cooled mount located between M3 and M4, showing the red circular TEM_{00} spot reflected on the ND glass filter of the powermeter head.

About 90% of the pump power was absorbed by the low-doped gain medium oriented for a π-polarized emission at λ_ω~1321nm (*c*-axis parallel to lasing *E*-field). A Faraday optical diode, consisting of a 20mm long Brewster-cut TGG rod and a zero-order half-wave plate (HWP), provided a robust unidirectional lasing without the ppKTP, as in the self-starting KLM Ti:Sa ring resonator demonstrated in Ref [29]. When the ppKTP is pulled out, both the forward clockwise (FW, from M3 to M4) and backward counter-clockwise (BW, dashed arrow at M3) lasing directions could be chosen with a proper rotation of the HWP. The Brewster-cut TGG rod facet further provided an additional more powerful output for the FH wave than the out-coupling HR mirror M3.

For cw SLM operation and tuning, a 100μm thin fused-silica etalon is placed right after the laser crystal in the near-field range of the bigger cavity waist so as to minimize diffraction loss, but under the dynamical regime described in Section 3 the etalon was removed. The ppKTP chip (grating period Λ~16.9μm, dimension 5 (W) × 1 (T) × 10 (l_c) mm^3, dual-band (1321/661nm) AR-coated, from Raicol Crystals Ltd) was positioned at the smaller cavity waist w_0. It was temperature-stabilized to ± 0.1°C by means of a Peltier cooler and one of its facets had a small wedge (~0.08 deg) in the (W) vertical direction to allow fine continuous SLM wavelength tuning over ~50pm via optical path length change when it is translated in the vertical direction. The measured total round-trip passive FH loss of the ring cavity amounted to L~3% without the ppKTP.

The small ($P_\omega \leq$ 15mW) IR power leaking through mirror M3 is used for diagnosis purposes. Part of it is sent to a scanning confocal Fabry-Pérot interferometer (CFP) with a free-spectral-range FSR = 750 MHz and finesse F = 60, and the remaining part to a near-IR wavemeter, to an optical spectrum analyzer (OSA), and to a fast DC-coupled InGaAs photodiode with ~50ps rise time (TeraHerz Technologies, model TIA-1200) connected to a 6-

#121572 - $15.00 USD Received 17 Dec 2009; revised 28 Jan 2010; accepted 29 Jan 2010; published 23 Feb 2010

GHz bandwidth digital oscilloscope. A small fraction of the red light exiting mirror M4 could also be directed to the OSA.

3. Partially mode-locked operation via cascaded Kerr nonlinearities

3.1 Optimally out-coupled fundamental SLM power at 1321nm

The FH laser oscillation was first characterized without the ppKTP. The Nd:YLF crystal could be pumped up to P_{abs}~14W of diode absorbed power at 806nm, before an abrupt thermal rollover occurred due to thermal negative lensing of the fluoride host [41]. Hence in what follows we have restricted the pump power to this upper limit to avoid any thermal effect. The highly reflecting mirror M3 (Fig. 1) was replaced with T = 0.5%,1%,2% and 4% output couplers and the distance M3-M4 reduced by ~4mm to bring the resonator at the mid-point of its stability range without the ppKTP so as to retrieve a TEM_{00} mode. Optimal out-coupling efficiency at maximum pump power was achieved with the T = 2% coupler, yielding P_ω = 1.6W of unidirectional power without any etalon (Fig. 2a), with a lasing on two longitudinal modes as analyzed by the scanning CFP and a pump threshold P_{th} = 2W. The IR beam quality factor of the laser mode was measured to be M^2 = 1.05 in both the horizontal and vertical planes. This power decreased to P_ω = 1.4W for single-frequency operation (trace 3 in Fig. 3a) with the insertion of a thin etalon with facets reflectance R = 25%. This SLM performance is identical to that of the σ-polarized laser (λ = 1314nm [7,8],), given the same saturation intensity of both σ and π transitions in Nd:YLF. A slightly larger SLM power (1.5W) could be obtained at gain center with an uncoated (R = 5%) etalon but wavelength tuning across the whole gain bandwidth as in Fig. 2b could not be achieved with this lower-contrast etalon due to a mode hop to the adjacent etalon fringe order beyond a certain tilt angle. So we kept for the FH optimal reference power the SLM output of 1.4W obtained using the R = 25% etalon, for comparison sake with the optimal SH power achieved in Section 4.

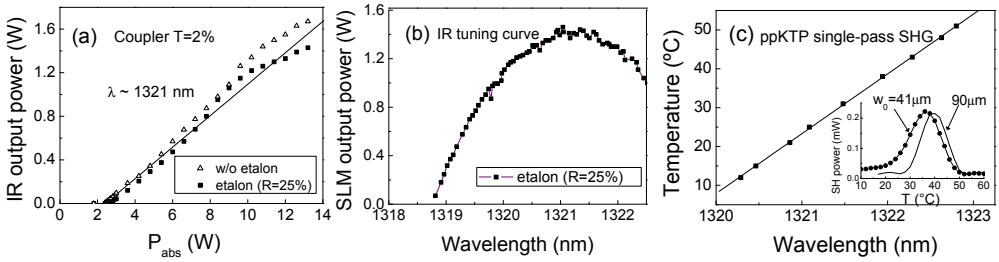

Fig. 2. (a) Optimally out-coupled FH power versus absorbed pump power, obtained with a T = 2% output coupler, without etalon (triangles, bi-modal lasing) and with a R = 25% etalon (squares, SLM operation); (b) FH SLM tuning curve; (c) ppKTP QPM temperature versus IR wavelength recorded under w_0 = 90μm loose focusing (inset: ppKTP temperature acceptance bandwidths at 1322.12nm for a loose focusing – w_0 = 90μm – and for a stronger focusing - w_0 = 41μm – showing a – 4°C QPM temperature shift characteristic of strongly focused SHG).

Without the ppKTP, the spectrum of the FH laser emission as analyzed by the OSA (resolution bandwidth ~0.02nm) is narrowband and centered at the maximum gain wavelength, λ~1321.3nm (Fig. 3b, trace 2). Plotted on the same graph (dotted) is the spectral bandwidth of the ppKTP, which position within the laser gain bandwidth is controlled by temperature according to the QPM tuning curve plotted in Fig. 2c. Temperature tuning allowed hence to vary the phase-mismatch ($\Delta k = k_{2\omega} - 2k_\omega - \pi/\Lambda$) experienced by the lasing modes near gain center without cavity misalignment. The cardinal-sine curve in Fig. 3b moves to the right when T>30°C (resulting in Δk>0, *i.e*. *defocusing* Kerr nonlinearity [22]) while for T<30°C it moves to the left (Δk<0, *i.e*. *focusing* Kerr nonlinearity).

#121572 - $15.00 USD Received 17 Dec 2009; revised 28 Jan 2010; accepted 29 Jan 2010; published 23 Feb 2010

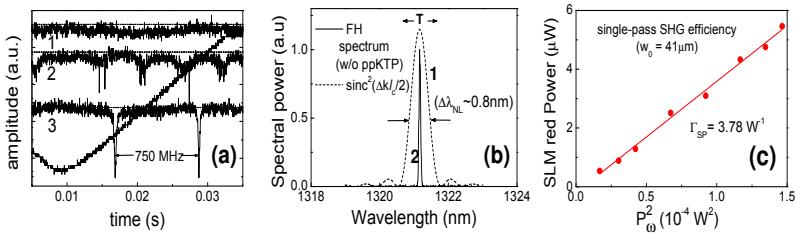

Fig. 3. (a) Scanning CFP transmission: Trace 3 corresponds to cw SLM (traces 1-2 are related to the dynamical pulsing regime in section 3.2 and section 4); (b) FH spectrum (solid line) without ppKTP (SLM or bi-mode). The dashed curve depicts the plane-wave QPM curve of ppKTP that can be shifted with temperature; (c) ppKTP single-pass efficiency $\Gamma = P_{2\omega}/P_{\omega}^{2}$.

With a small fraction of the SLM FH power (~15mW), the ppKTP phase-matching properties were characterized at λ = 1321.3nm in single-pass SHG versus temperature, using various focusing conditions characterized by the focusing parameter $l = l_c/z_R$ [8], where $z_R = k_\omega w_0^2/2$ is the beam internal Rayleigh length (Fig. 2c). Under plane-wave focusing (l<<1 with w_0 = 90μm), the phase-matching temperature corresponding to gain center oscillation (λ_ω ~1321.3nm) was measured to be T~38°C (with an acceptance bandwidth ΔT = 10°C). The ppKTP tuning slope versus temperature (Fig. 2c) was determined to be $d\lambda_\omega/dT$ = + 0.066nm/°C for a temperature range between + 15°C and + 75°C (covering the FH emission bandwidth). At a stronger focusing (w_0 = 41μm, a value comparable to the intracavity waist), the QPM temperature (T~34°C) is shifted by –4°C due to focusing effects and the bandwidth is slightly broadened (inset of Fig. 2c), displaying an asymmetric profile (at strong focusing, optimal SHG conversion is obtained at $\sigma = \Delta k z_R$ ~-0.2 and not at σ = 0 [16,43]). The net measured single-pass conversion efficiency at w_0 = 41μm (using a calibrated Si pin photodiode) was $\Gamma_{SP} = 3.8 \times 10^{-2}$ W/W^2 (Fig. 3c), after correction of the the ~21% transmission loss factor of two KG5 Schott glass filters blocking the FH wave. The experimental QPM spectral bandwidth was roughly measured to be $\Delta\lambda_{NL}$≈0.8nm (FWHM) by mode-hop tuning the laser.

3.2 Self-starting self-pulsing dynamics upon ppKTP insertion: Observations

For the ICSHG laser, the distance M3-M4 was reset to the value given in Section 2 so that the cavity operated again at η ~0 in presence of the ppKTP and the T = 2% output coupler was replaced with a HR mirror. Prior to the insertion of the ppKTP, the mode spectrum analyzed by the scanning CFP displayed again oscillation on 2 longitudinal modes centered at gain maximum (λ~1321.3nm from the wavemeter display). The corresponding OSA spectrum is narrow as expected (trace 2 in Fig. 3b). Owing to the measured T~1/4500 transmittance of M3 and the ~15mW leakage through it, the maximum estimated unidirectional intra-cavity power amounted to P_{cav}~67.5W.

When either a critically-phase matched (CPM) LBO or BiBO crystal was inserted *in lieu* of the ppKTP, SLM oscillation is also spontaneously achieved without any etalon owing to the well-kown nonlinear self-suppression of adjacent longitudinal modes in cw ICSHG lasers [44]. With a type-I(ooe) cut BiBO, up to 650mW of cw SLM red power was easily obtained at line center [8] with a laser spectrum identical to that shown in Fig. 3b. The scenario turned to be quite different when the ppKTP was inserted into the ring cavity with its temperature set to T~30°C corresponding to QPM (Δk~0) of the maximum-gain wavelength (Fig. 2c).

#121572 - $15.00 USD Received 17 Dec 2009; revised 28 Jan 2010; accepted 29 Jan 2010; published 23 Feb 2010

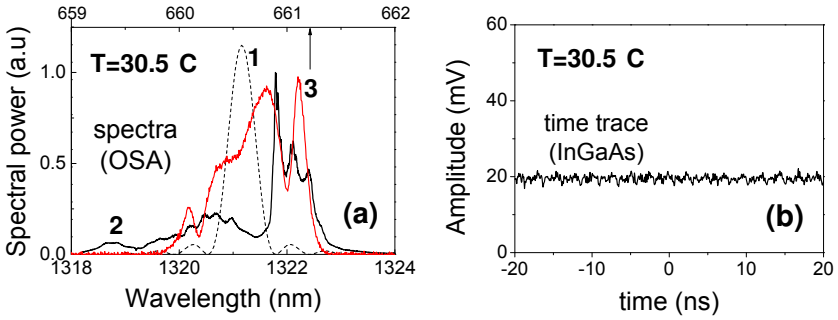

Fig. 4. (a) FH (2) and SH (3) broadest spectra recorded at T = 30.5°C, when the ppKTP is quasi-phase-matched at gain-center wavelength along with the position of the spectral SHG curve (1) at T = 30.5°C. The inset displays the temporal trace of the InGaAs photodiode; (c) Corresponding temporal FH trace recorded by the fast InGaAs detector (no self-pulsing observed at T~30°C).

Surprisingly with ppKTP, the usual longitudinal mode spectrum disappeared and practically no FH light was transmitted by the CFP interferometer (Fig. 3a, trace 1). Concomitantly the display of the wavemeter became erratic. These two facts actually triggered our suspicion that a broadband laser emission was at stake, requiring a more specific temporal and spectral diagnoses. Traces 2 and 3 in Fig. 4b displays the stunning spectral gain broadening in the FH and SH spectral ranges as compared with the narrow-line spectrum of the FH laser before the ppKTP insertion (Fig. 3b), while strikingly no pulsing is detected by the InGaAs detector (Fig. 4b). The spectra shown in Fig. 4a, corresponding to the broadest recorded ones – extending over the full fluorescence bandwidth of the π-polarized transition [8] –, were recorded only near T~30.5°C. The fact that the DC background signal detected by the InGaAs (Fig. 4b) could not interfere in the scanning CFP meant that the broad emission is phase incoherent (white light continuum). Let us note that the SH spectrum shown in Fig. 4a extends far beyond the spectral QPM curve (dashed $\mathrm{sinc}^2(\Delta k l_c/2)$ curve 1), meaning that SH conversion arises even for wavelengths experiencing large phase-mismatches. Such spectral gain broadening is manifestly due to nonlinear self-phase modulation brought by the ppKTP, via $\chi^{(2)}$:$\chi^{(2)}$ cascading processes.

As already pointed out, changing the ppKTP temperature controls the amount of wave vector mismatch $\Delta k(\lambda_\omega,T)$ experienced by the lasing modes nearby the laser gain maximum. When the ppKTP spectral acceptance curve was tuned away from T~30°C, a high contrast (up to 70%) pulse train at f_{rep}~420 MHz was recorded by the fast photodiode in correlation with a variety of narrower spectral emission bandwidths (Fig. 5). The periodic (f_{rep} = 2.4ns) self-pulsing behavior was observed at any temperature (corresponding to both negative and positive Δk), except near T~30°C for which $\Delta k(\lambda_\omega)$~0 (Fig. 4b). This contrasts with CSM for which mode-locking was found to occur only at higher ppKTP temperatures corresponding to the defocusing cascaded Kerr nonlinearity, within an extremely limited pump range in the thermal rollover region [21]. From Fig. 5d, pulse trains characterized by the absence of satellite pulses develop at the largest positive (defocusing [22]) phase-mismatch, while at negative (focusing [22]) mismatch (Fig. 5a) some satellite pulses were observed. From Fig. 5, one can also notice that the DC background level on the temporal traces increases for defocusing Kerr nonlinearity. Recording the same spectra at the output of M4 (*i.e. after* passing the ppKTP) yielded nearly identical shapes except that the fast modulations observed on the FH traces were more pronounced, evidencing that the pulses were not in the solitonic regime characterizing a full KLM mode-locking process. The pulse width in Fig. 5d was measured to be τ~250ps from the oscilloscope trace. We believe that this measured width is not instrumentation-limited since the InGaAs photodiode rise time was ~50ps, compatible with the sampling time interval of the digital oscilloscope. Hence the pulses are far from being transform-limited, which justifies the "partial KLM" labelling attributed to the ultra-fast self-pulsing behavior.

#121572 - $15.00 USD Received 17 Dec 2009; revised 28 Jan 2010; accepted 29 Jan 2010; published 23 Feb 2010

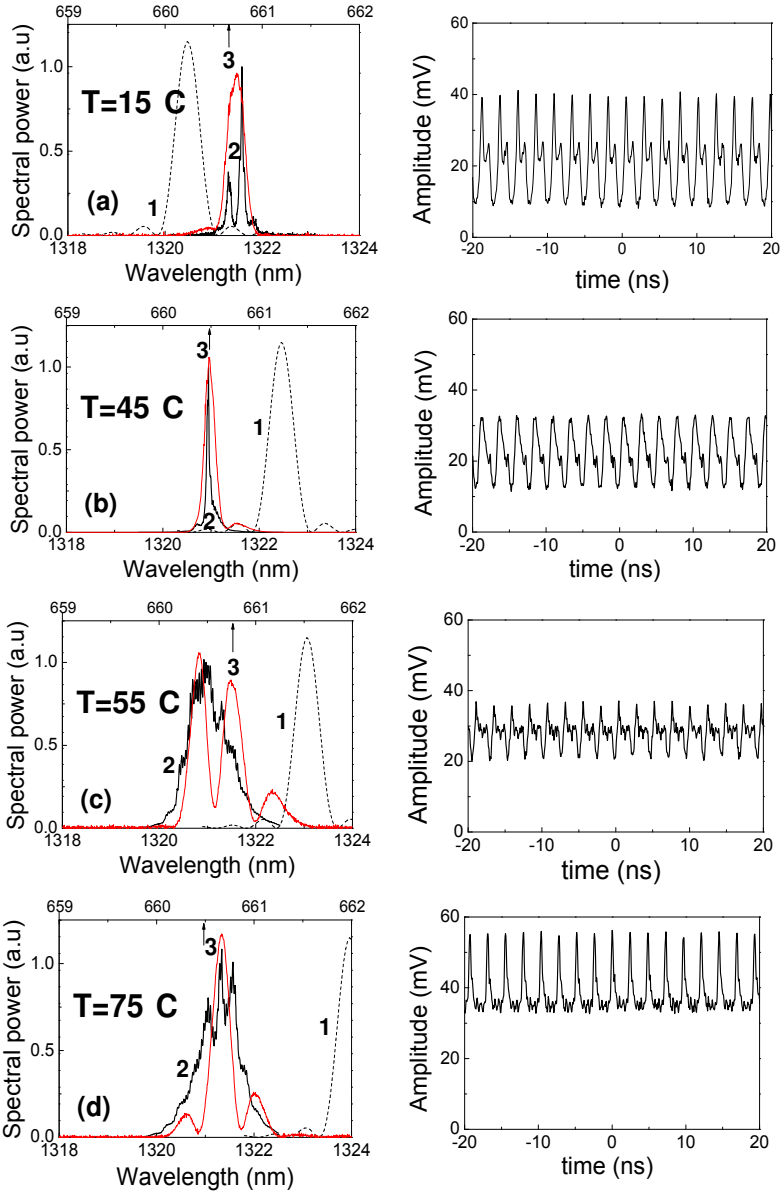

Fig. 5. . FH (2) and SH (3) spectra (left panels) and correlated FH time traces (right panels) recorded at various ppKTP temperatures on the focusing Kerr nonlinearity side (T = 15°C, top panel) and on the defocusing Kerr nonlinearity side (T = 45°, 55°, 75°C, lower panels). The pump power was P_{abs} = 13W. The temperature-shifted QPM curve is also shown with dashed lines (1).

We have also recorded the pulse train and spectra evolution at a fixed temperature as a function of the input pump power, to check whether a threshold in terms of intracavity power could be evidenced. Figure 6 displays such a recording at T = 70°C. As the pump power is decreased, the scanning CFP output pattern gradually shifts from "no transmission" (trace 1 in Fig. 3a), an intermediate noisy pattern such as in trace 2 and finally a clear narrow fringe pattern such as in trace 3 as the background DC level retrieves its phase-coherence and narrow-band cw properties in the last panel row (P_{abs} = 6.5W). This pump level corresponds to a circulating FH threshold intensity of ~1MW/cm^2 at the ppKTP focus. The FH spectrum

#121572 - $15.00 USD Received 17 Dec 2009; revised 28 Jan 2010; accepted 29 Jan 2010; published 23 Feb 2010

displays then a main narrow line containing actually two longitudinal modes beating at FSR_{cav} (the temporal waveform is nearly sinusoidal). This observation tends to support the assumption that the KLM dynamics recorded at higher pump power is initiated spontaneously by longitudinal mode-beating intensity noise, without the need of an external perturbation such as in most KLM lasers. The role of the unidirectional ring configuration avoiding etalon effects may also explain the self-starting nature of the pulsing dynamics [29–32], since such dynamics were not reported *e.g*. in other cw standing-wave ICSHG lasers employing thick ppKTP [34,35] or PPLN [37] crystals.

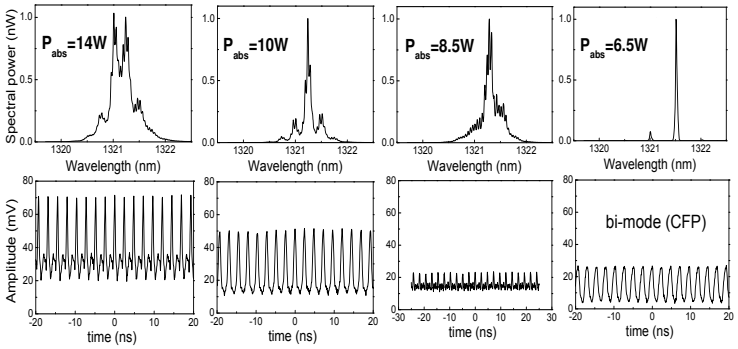

Fig. 6. FH Spectra and time traces at T = 70°C as function of the diode pump decreasing power. The bottom panels display the relative amplitude of the pulse train. At P_{abs}<6.5W the spectral gain broadening disappear and the laser recovers narrowband cw operation (bi-modal regime as checked with the CFP interferometer).

The temporal pulse trains were also recorded on longer (microsecond) time scales and their envelope studied as a function of the ppKTP temperature (Fig. 7). The pulse trains were not stationary as in a fully (solitonic) mode-locked laser for which a 100% pulse contrast is observed, but displayed either a random intensity-modulated envelope or sometimes a Q-switched like envelope. In general, the pulse waveforms and spectra depended on both the pump power and the ppKTP temperature. Although no clear picture could be established, the largest pulse contrast (~70%, Fig. 5a) seemed to correspond to low ppKTP temperatures (T<30°C, self-focusing) while the shortest pulse width (first row in Fig. 6) occurred rather on the defocusing Kerr nonlinearity side (Δk>0, T~70°C). In all cases the pulse repetition rate was extremely stable in time as recorded with a RF spectrum analyzer. From the inspection of Figs. 4-5, a necessary condition for partial KLM operation is a substantial wave-vector mismatch experienced by the ppKTP whichever the sign of the Kerr nonlinearity. The most stationary waveform we were able to record at T = 20°C is shown in the last panel of Fig. 7.

The details of the pulse waveform corresponding to the last panel in Fig. 7 also shows some satellite secondary pulses (Fig. 8a) characteristic of a non perfect (affected by self-phase modulation and frequency chirping) mode-locking process. Frequency chirping due to SPM may also account for the broadband incoherent DC background level that cannot interfere inside the scanning CFP. Although the pulse content is expected to carry a phase-coherent signal, the lack of time synchronism between the pulse repetition rate (f_{rep}~420 MHz) and the CFP free-spectral range (FSR = 750 MHz) would prevent any constructive interference within the CFP interferometer, hence the quasi-null transmission of the latter (trace 1 of Fig. 3a).

#121572 - $15.00 USD Received 17 Dec 2009; revised 28 Jan 2010; accepted 29 Jan 2010; published 23 Feb 2010

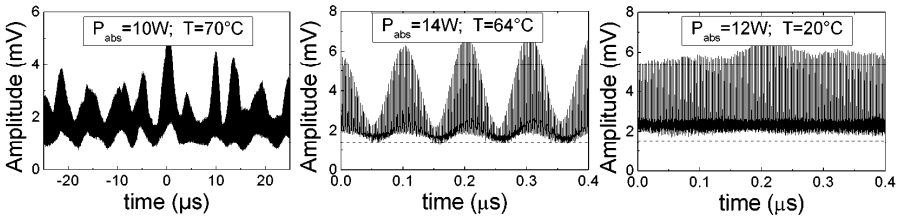

Fig. 7. Pulse train envelopes recorded at microsecond time scales. The envelope pattern varies not only versus the ppKTP temperature but also depends on the diode pump power. The horizontal dashed lines in the two last panels indicate the level of cw (narrow band) output from the laser when the ppKTP is translated out of the cavity.

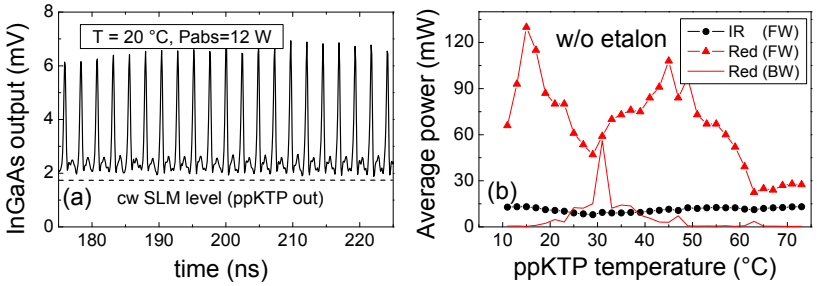

Fig. 8. (a) A close-up shot of the central part of the temporal waveform in Fig. 6 (T = 20°C). The dashed line gives the cw coherent level detected by the InGaAs when the ppKTP is removed from the cavity (narrow CFP fringes are detected in this case). (b) Red power exiting in both directions (forward and backward) as a function of ppKTP temperature, without any etalon and at P_{abs} = 13W. The black circle data are the FW fundamental power leaking through M3.

Other additional observations have to be reported for completeness sake. We noted that an axial translation by ± 3mm of the ppKTP crystal (limited by the mini-translation stage travel, Fig. 1b) around the waist between M3 and M4 changed only weakly the spectral or temporal patterns of the emission. Such a relative insensitivity is in contrast with the critical position of the $\chi^{(3)}$ thin medium in KLM resonators [25,31]. However the spectra shapes or the pulse contrast may depend on slight ring cavity misalignments, which could be attributed to slight change the intracavity intensity. It is also worthwhile mentioning that the insertion of the ppKTP slightly disturbed the strong unidirectional lasing of the FH ring cavity. Starting from a perfect adjustment of the HWP rotation of the optical diode so as to maximize the FH power and the uni-directionality, the insertion of the ppKTP caused systematically a weak bi-directional lasing (with a BW:FW ~1:10 intensity ratio of the counter-propagating waves, the weak BW travelling-wave exiting from M3 along the dashed arrow shown in Fig. 1). Strictly uni-directional lasing could not be retrieved by rotation of the HWP controlling the optical diode isolation against backward oscillation. Periodically-poled crystals may behave as Bragg-reflecting intracavity elements in ring lasers, causing a strong backward counter-propagating oscillation due to the small index discontinuities at the domain walls [45], but this explanation in our case is ruled out by the fact that under cw SLM operation (see next section), the ICSHG laser retrieves a perfect uni-directionality. Although the origin of this intriguing weak bi-directionality under the dynamical regime is not fully understood, a tentative explanation is that the nonlinear cascaded phase shift may strongly affect the phase of the circulating FW wave, resulting in imperfect directional loss discrimination of the optical diode. In this experiment, a faint cw red beam was then generated along the backward direction. It is important to emphasize however that the FW pulsing red wave exiting the ppKTP is in no way reflected back to the nonlinear crystal as in NLM [17–21] or CSM

#121572 - $15.00 USD Received 17 Dec 2009; revised 28 Jan 2010; accepted 29 Jan 2010; published 23 Feb 2010

[15,16] mode-locking owing to the ring configuration: The R~10% forward travelling red beam reflected by M4 escapes totally through M2 and is not re-injected into the ppKTP. In other words, the intracavity SHG process is purely of a single-pass kind and the self-starting partial mode-locking mechanism at stake is a based on pure KLM effects triggered by an additional $\chi^{(3)}$ nonlinear medium (different from the gain medium itself [29,30]) such as in the first Nd:YLF laser mode-locked by a SF57 glass rod [26,28], although in these works the use of an intracavity slit was required together with operation of the cavity near the stability boundary due to the weakness of the genuine $\chi^{(3)}$ nonlinearities.

It is instructive to inspect the recorded red power exiting both along the FW direction (partially mode-locked) and along the BW direction (cw regime) as function of the ppKTP temperature at P_{abs} = 13W (Fig. 8b). The occurrence of pulsing only in the FW propagation direction corroborates the results that ring cavities favor self-starting unidirectional KLM operation, owing to the asymmetry of the small amplitude gain modulation even without an optical diode [29–32]. Interestingly while the weak BW propagating red beam (solid red line in Fig. 8b) sketches as expected the temperature-tuning curve of the ppKTP, with a peak power nearby the center gain wavelength (T~30°C), the stronger (pulsing) FW generated red power displays a dip at this "optimal" temperature and two broad maxima at T~15°C and T~45°C. Reminding that at T~30.5°C (Δk~0) the FW beam is extremely broadband and phase incoherent (Fig. 4a), the red minimum observed near this temperature is not a surprise. By contrast the two red power maxima in Fig. 8b coincide with the highest pulse contrast (Figs. 5a-b). The overall amount of broadband red light generated in the FW direction under partial KLM operation did not exceed P_{red}~150-250mW, far less than under cw SLM regime (Section 4). The low SHG efficiency arising from the phase-coherent pulse content (at T~15°C and T = 45°C) cannot be explained – given the long ~250ps duration of the pulses – by the group velocity mismatch (GVM) between the FH and SH pulses inside the long ppKTP [16] (note that in a ring cavity the effect of GVM is half that in a standing-wave one). This SHG inefficiency is rather attributed to the large phase-mismatch at these temperatures, as witnessed by the position of cardinal-sine functions in Fig. 5. The FW red power displayed in Fig. 8b is also quite different from the bistable behavior of the green Nd:YAG/ppKTP output power against temperature recorded by Greenstein *et al*, who did not observe these KLM dynamics in their Z-fold standing-wave resonator [34].

3.3 Qualitative analysis of the partial KLM process

Given the $\Delta\lambda_G$ ~4nm FH spectral emission in Fig. 4a and the FSR_{cav} = 420 MHz of the ring cavity, more than 3,500 longitudinal modes are simultaneously oscillating once the ppKTP is inserted near T~30°C. This self-broadening process is undoubtedly due to nonlinear self-phase and cross-phase modulation or other effective third-order scattering processes occurring inside the ppKTP. The estimation of the maximum circulating FH power yields P_ω~70W, corresponding to an intensity $I_\omega = P_\omega/(\pi w_0^2/2) \approx 2$ MW/cm^2 at the ppKTP crystal. While such a moderate power density excludes genuine $\chi^{(3)}$ KLM effects, the ~3 orders of magnitude larger effective Kerr nonlinearity brought by cascaded $\chi^{(2)}$: $\chi^{(2)}$ processes [22,23] can explain the partial KLM dynamics observed without the enhancement of nonlinear loss modulation required in standard KLM or CSM lasers brought by setting the ring cavity at the first boundary of its stability range ($\eta \rightarrow$-1). These effective $\chi^{(3)}$ nonlinearities can results in giant nonlinear index of refraction, $n_2 I_\omega$ responsible of Kerr focusing (or defocusing) effects (the sign of n_2 is opposite that of Δk [22]) and self-and-cross phase modulation of longitudinal modes via cascaded sum-and-difference frequency processes. For a single-pass SHG with no SH input, the usual plane-wave coupled-wave equations describing the exchange of energy between $E_\omega(z)$ and $E_{2\omega}(z)$ (where E_j denote the slowly varying field amplitudes) are equivalent to [22,46]

$$\frac{d^2E}{dz'^2} + i\Delta k l_c \frac{dE}{dz'} - \Gamma^2 l_c^2 \left(1 - 2|E|^2\right) E = 0 \qquad (1)$$

#121572 - $15.00 USD Received 17 Dec 2009; revised 28 Jan 2010; accepted 29 Jan 2010; published 23 Feb 2010

where the FH field amplitude $E_\omega(z)$ has been normalized to its initial value $E_0 = E_\omega(0)$ such that $E = E_\omega/E_0$ ($\gamma = |E|^2$ measures hence the FH depletion factor) and the physical longitudinal variable z is normalized as $z' = z/l_c$. The nonlinear coupling constant Γ expresses as $\Gamma = \omega d_{\text{eff}} |E_0| / c\sqrt{n_{2\omega} n_\omega}$ (in m^{-1}). The cubic field term proportional to $|E|^2E = E^2E^*$ in Eq. (1) is responsible of cascaded Kerr effects, specifically $\chi^{(2)}(-2\omega;\omega,\omega)$: $\chi^{(2)}(-\omega;2\omega,-\omega)$ in the case of SHG. In Fig. 9 we have numerically solved Eq. (1) by writing $E(z) = \sqrt{\gamma}\exp(-i\varphi_{NL}(z))$ using the experimentally relevant parameters ($\Gamma^2 l_c^2 = 0.46$ by using $d_{\text{eff}} = 9$pm/V [42]).

A maximum nonlinear phase-shift (NLPS) $|\varphi_{NL}|_{max} = 0.13$rad is achieved at $\beta = \Delta k l_c = \pm \pi$. Such a rather small value is apparently enough to trigger the cascaded Kerr dynamics. For $|\Delta k| >> \Gamma$ the NLPS can be approximated as $\phi_{NL} \approx -\Gamma^2 l_c^2 / \Delta k l_c$ [22] from which an effective intensity-dependent nonlinear index $n_2 I$ (such that $n = n_0 + n_2 I$) can be expressed with the definition $\phi_{NL} = (2\pi l_c / \lambda) n_2 I(r,t)$. From Fig. 9b showing the evolution of the NLPS inside the nonlinear medium, it actually improper to define a uniform nonlinear index since $\varphi_{NL}(z)$ varies with z. However an average estimation of nonlinear index of refraction at $|\beta| = \pi$ yields $n_2 = \pm 1.45 \times 10^{-12}$ cm^2/W (depending on the sign of Δk), already ~3 orders of magnitude larger than in $\chi^{(3)}$ media. In his theoretical analysis of KLM ring resonators [31], Agnesi has shown that the small-signal Kerr nonlinear gain $\Delta g(z)$ in ring resonators is not only asymmetric with respect to the counter-propagating directions but also scales as $\pm n_2 / (1 - |\eta|)^{1/2}$.

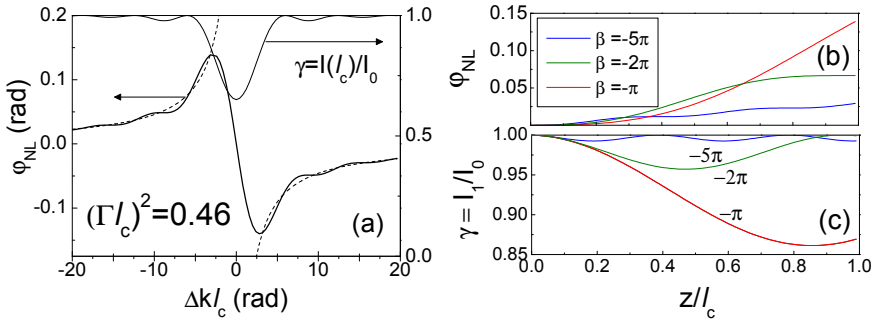

Fig. 9. . (a) Cascaded second-order nonlinear phaseshift for $I = 2 \times 10^{+6}$ W/cm^2 versus the phase-mismatch parameter (solid line). The dotted line is the analytical approximation given in [22]. The thin upper curve is the FH depletion factor. (b) Nonlinear phase-shift (NLPS) versus the position z inside the ppKTP, for various phase-mismatch parameters $\beta = \Delta k l_c$. (c) the corresponding evolution of the FH intensity depletion and NLPS versus z. For even integer value of β/π the energy flows periodically from the FH to the SH and backward and the net SH conversion is nil at the output of the ppKTP.

The 3 orders of magnitude larger n_2 stemming from $\chi^{(2)}$:$\chi^{(2)}$ cascading compensates for the fact that our ring cavity operates at η ~0, which is in principle not the ideal condition for self-starting hard-aperture KLM as analyzed by Magni *et al* in terms of the maximum achievable relative spot size variation with intracavity pulse power [36]. However, the theoretical KLM resonator analysis of Brabec *et al* [25] considering an X-fold 4-mirror cavity geometry identical to ours evidenced that while the condition $|\eta| \rightarrow 1$ apply to hard-aperture KLM resonators, in soft-aperture longitudinally-pumped solid-state lasers, the maximum power-dependent amplitude modulation occurs rather at the middle of the stability range of the resonator (η ~0), without any practical demonstration to date. Our experiment tends hence to confirm this result when the effective Kerr nonlinearities is strong enough.

An interpretation of the pulsing dynamics in terms of partial KLM mode-locking mechanism can be provided based on the generalized ABCD matrix formalism taking into account intracavity Kerr focusing or defocusing effects [47]. In passively mode-locked KLM

#121572 - $15.00 USD Received 17 Dec 2009; revised 28 Jan 2010; accepted 29 Jan 2010; published 23 Feb 2010

or CSM lasers, the self-focusing or defocusing effects must be associated with a power-dependent gain and loss mechanisms in order to sustain a stable train of pulses, the loss mechanism being usually provided by either an intracavity *hard* or a *soft* aperture [16,25,31,32]. When the cascaded Kerr nonlinearity is focusing at the ppKTP (equivalent of an increase of M3-M4 distance in the linear cavity), the FH transverse mode waist at the Nd:YLF increases rapidly, inducing a loss for the TEM_{10} mode at the benefit of the TEM_{00} mode as discussed at the beginning of Section 3.2. For defocusing nonlinearity (equivalently a decrease of M3-M4), the cavity waist at the gain medium shrinks instead in favor of the TEM_{10} mode. Hence whichever the Kerr nonlinearity sign as predicted by Heatley *et al* [32], a power-dependent gain-loss mechanism exists that leads to pulse formation. This may explain why the pulsing dynamics does not depend on the ppKTP temperature. The Q-switched periodic envelope sometimes modulating the pulse train (Fig. 7) may further arise from transverse TEM_{00} and TEM_{10} mode-beating.

Finally to end this section, let us mention that – if the interpretation of the pulsing dynamics in terms of partial KLM process holds (we leave this issue cautiously opened) – it should be possible to obtain (as in $\chi^{(3)}$ medium-based KLM lasers) a fully self-starting mode-locked ICSHG laser in the ps/sub-ps regime from this Nd:YLF/ppKTP ring laser by, *e.g*., optimizing the curved-mirror spacing (so that $|\eta|\rightarrow 1$), and eventually by compensating the GVM between the FH and SH shortening pulses in the ppKTP crystal [15,16]. However, since the both FH and SH have the same polarization (the QPM type is *eee* rather than *oeo*) another technique than the insertion of a birefringent phase plate has to be used. Additional experiments regarding the role played by the intra-cavity optical diode, the influence of the ring versus standing-wave geometry (in the latter case confusion with NLM or CSM may rather complicate the interpretation) and the importance of the ratio $\gamma = \Delta\lambda_{NL}/\Delta\lambda_G$ (it would be interesting to repeat our experiment on the much stronger but also narrow 1.05μm transition) are needed to ascertain our finding.

4. Cw single-frequency operation: an optimally-coupled Nd:YLF/ppKTP ICSHG laser

In this last section, we shall describe the transition from partial KLM regime to cw tunable SLM regime, *i.e*. how we could achieve SLM operation of the ICSHG laser despite the strong Kerr-lens dynamics reported so far.

Obtaining cw SLM regime with optimal SHG efficiency by starting from the partial KLM regime was found quite difficult and calls not only for the insertion of a suitable frequency-selective etalon but also for the delicate adjustment of various parameters. The key issue was to find a way to force the SLM mode (prior to ppKTP insertion) to experience the smallest possible phase-mismatch once the ppKTP is inserted, given the fact that the finite bandwidth of the QPM process with regards to the laser gain bandwidth may lead to oscillation on longitudinal modes not necessarily matching the peak of the nonlinear spectral bandwidth [33]. Greenstein *et al* have shown in a simple theoretical model derived from Smith [14] that when the ratio $\gamma = \Delta\lambda_{NL}/\Delta\lambda_G < 1$ (in our case $\gamma \sim 0.2$), it is difficult to achieve the regime of optimal SHG conversion in homogeneously broadened ICSHG lasers and that multi-longitudinal mode operation is always expected. The explanation can be summarized as follows. At low pump rate or low SHG nonlinearity, the roundtrip linear loss is dominant and the laser oscillates SLM on the mode closest to the gain-center wavelength, and other modes are suppressed by the spontaneous nonlinear self-suppression mechanism of longitudinal modes via increased SFG loss [44]. Increasing the gain or the SHG nonlinearity to the point where the nonlinear loss becomes dominant for the SLM mode, the net gain profile reveals then spectral regions (at non nil $\Delta k(\lambda)$) where longitudinal modes can overcome the nonlinear SFG loss, leading to multi-mode oscillation and in our case to the Kerr-lens dynamics. Hence the finite QPM bandwidth, as opposed to $\gamma > 1$ for most of the birefringence phase-matched crystals [8], is an obstacle to achieve the optimal conversion SLM regime as predicted by earlier theories of ICSHG lasers [13,14]. To overcome this difficulty, a spectrally selective etalon must be inserted to enforce SLM operation with the smallest Δk. However the

#121572 - $15.00 USD Received 17 Dec 2009; revised 28 Jan 2010; accepted 29 Jan 2010; published 23 Feb 2010

additional loss introduced by the etalon must be moderate if the optimal ICSHG regime were targeted.

In our previous work reporting on the σ-polarized laser (1314nm) [7], a maximum of 1W SLM red power at 657nm was achieved relatively easily by using a high-reflectance (R = 40%) thin etalon that efficiently quenched the cascaded second-order processes. In this work, we tried to use the lowest-contrast (uncoated) fused-silica etalon (R~4%), but could not get rid of the pulsing dynamics for any angular position. So an intermediate partially R-coated (R = 25%) etalon was further tried.

Starting from maximum pump power with the ppKTP translated out of the cavity, the angular position of the etalon was first adjusted to obtain easily SLM fundamental oscillation at the central-gain wavelength (~1321.3nm). But upon the ppKTP (set to T~30°C) insertion the gain broadening and KLM dynamics could not be quench automatically because the insertion, by modifying the cavity optical path length, changed also the wavelength value by ± 0.1 to ± 0.2 nm, leading to a mixed temporal regime characterized by a CFP transmission as shown in trace 2 of Fig. 3a. By tilting further the etalon and translating vertically the ppKTP along its wedged facet direction, specific etalon/ppKTP positions could then be found for which SLM lasing is retrieved, with a simultaneous burst of the usual sharp CFP fringes (trace 3 in Fig. 3a) and a sudden jump in the detected red power from ~150mW (Fig. 8b) to some hundreds of mW. Simultaneously the weak cw counter-clockwise (BW) beam detected behind M3 disappeared, restoring a perfect unidirectional operation of the ring laser. This last observation definitely proves that the weak bidirectionality observed under partial KLM was induced by the cascaded NLPS. However, the new position of the etalon did not necessarily maximize the SLM red power. Slight vertical translation of the ppKTP along its wedge (to fine tune the oscillating SLM wavelength without inducing a mode hop) jointly with slight adjustment of the ppKTP temperature improved then gradually the detected SLM red power, in conjunction with small axial (z) translation adjustment of the ppKTP around the cavity waist, Then a small tilt is applied again to the etalon to check if the red power was maximum, taking care that the tilt amplitude was low enough so as not to induce back the partial KLM regime. The above procedure had to be iterated several times until the red SLM power was stationary around its maximum: At 1321.3nm we could ultimately achieve 1.4W at 660.65nm (the same optimal SLM fundamental power achieved in Fig. 2a), when corrected for the 10% reflection loss from the dichroic mirror M4. *A posteriori*, we found that another simpler procedure was to start from a pump power below the threshold for partial KLM (P_{abs}~6.5W, Fig. 6) and ramp gradually the pump power while adjusting the etalon and ppKTP positions in order to adiabatically track SLM oscillation versus P_{abs}, although during the adiabatic procedure a sudden transition to partial KLM regime may occur, witnessed by an instantaneous disappearance of the CFP fringes. Surprisingly, when maximum red SLM power is achieved, the laser can run single-frequency (with a stable wavelength readout) for more than an hour with less than 2% of red power decrease. However each time the ICSHG laser is switched off, the whole SLM retrieval procedure has to be started again to achieve the optimal red power. Figure 10b displays the maximum red power versus the absorbed pump power (1.4W at P_{abs} = 15W when corrected for the 10% reflection loss from mirror M4) achieved at gain-center wavelength. This power represents a 40% increase when compared to the maximum red SLM power achieved on the σ-polarized (1314nm/657nm) ICSHG laser employing a more selective (and lossy) R = 40% partially-coated etalon, resulting in a less problematic SLM operation [7]. Owing to the identical emission cross-sections of the 1314nm and 1321nm transitions, an equivalent power should be achievable at 657nm with a R = 25% etalon to probe the Ca ($^1S_0$– $^3P_1$) inter-combination line.

Polloni and Svelto first addressed in 1968 the theory of optimal-coupling in single-frequency ICSHG lasers starting from the 3 or 4-level laser rate equations including a quadratic nonlinear loss and neglecting any thermal effects [13]. It is convenient to re-express Polloni's rate equation results in terms of the saturation intensity of the 1.32μm transition $I_{sat} = h\nu / \sigma\tau$ (= 6.7kW/cm^2 [10]), the number of times $x = P_{abs}/P_{th}$ the laser is

#121572 - $15.00 USD Received 17 Dec 2009; revised 28 Jan 2010; accepted 29 Jan 2010; published 23 Feb 2010

pumped above threshold, and a non-dimensional nonlinear parameter $y = \kappa I_{sat} / L$. The scaled parameter y represents the ratio of nonlinear loss at $I_\omega = I_{sat}$ to the roundtrip passive loss L.

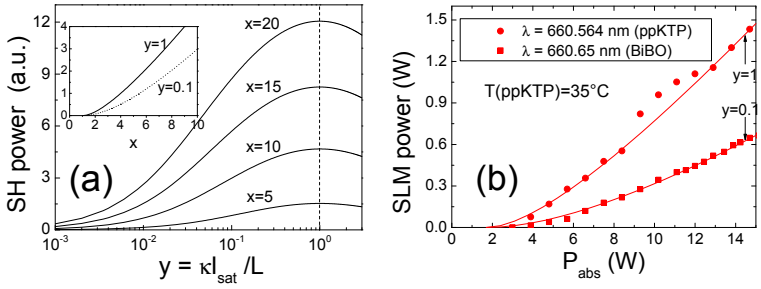

Fig. 10. (a) Theoretical ICSHG conversion efficiency plotted as function of the nonlinear y-parameter, showing that optimal conversion is achieved for $y_{opt} = 1$ independently of the pump parameter $x = P_{abs}/P_{th}$. The inset shows the SHG power as the pump is increased, for two values of y. (b) Experimental optimal SLM red power achieved at gain-center with ppKTP (circles), as compared with that achieved with a type-I cut BiBO. The solid lines are a fit to Eq. (2), yielding $y = 1.0$ (ppKTP) and $y = 0.1$ (BiBO).

The nonlinear coefficient $\kappa = (4\pi^2 / \varepsilon_0 c \lambda_\omega^2)(d_{eff}^2 / n^3)(l_c w / w_0)^2 G(\sigma)$ (in cm^2/W) in the definition of y is the strength of the SHG nonlinearity, where d_{eff}^2 / n^3 is the nonlinear figure-of-merit of ppKTP, w/w_0 is the ratio of the waists at the gain medium and at the nonlinear crystal, and $l_c G^{1/2}$ is the effective interaction length of the SHG crystal. For a standing-wave resonator an additional multiplicative factor β ($2<\beta<4$) has to be added to the definition of κ [10,14]. The aperture function G of the normalized wavevector mismatch $\sigma = \Delta k\, z_R$ accounts for focusing effects (and eventually for spatial walkoff), and is related to the usual Gaussian beam focusing function $h(\sigma)$ by $G \equiv 2h/l$ where $l = l_c/z_R$ is the focusing parameter [8,48]. For plane-wave focusing ($l \to 0$), one has $G(\sigma) \to \mathrm{sinc}^2(\Delta k l_c/2)$. Using these notations, the SH power for a 4-level transition can be cast as

$$P_{2\omega} = \frac{I_{sat}(\pi w^2 / 2)}{4y}\left[\sqrt{(y-1)^2 + 4yx} - (y+1)\right]^2 . \qquad (2)$$

Let us note that Eq. (2) is not valid for a 3-level laser [13], and we have checked its full compatibility with Eq. (8) of Smith [14] expressed with different normalized parameters and derived by equating the saturated gain to the sum of linear and nonlinear loss. It is worth mentioning that the Smith's rescaled formula (in terms of physically measurable quantities) given in [10] for a standing-wave ICSHG laser contains a typographical sign error in the term $(y\text{-}1)^2$ under the square-root symbol (a "+" sign appears erroneously in Eq. (1) of Ref [10].).

Optimal SH power can be derived from Eq. (2) by maximizing the r.h.s. with respect to y, yielding $y_{opt} = 1$ independently from the pump parameter x (Fig. 10a), meaning that the optimal SHG coupling condition depends only on the spectroscopic properties of the gain medium and on the strength of the nonlinearity – that can be varied either by choosing a highly nonlinear medium or a sufficiently long crystal (note that this optimum is rather shallow due to the semi-logarithmic scale in Fig. 10a). The fact that this condition does not depend on the pump parameter contrasts with the optimal coupler transmission of the FH laser (without SHG), $T_{opt} = L(\sqrt{g_0 l_G / L} - 1)$, which *does* depend on the pump parameter via the small signal gain coefficient g_0 [14]. This peculiarity stems from the quadratic intensity dependence of the SHG loss. By replacing y with $y_{opt} = 1$ in Eq. (2), one obtains $P_{2\omega}^{max} = I_{sat}(\pi w^2/2)L[\sqrt{x} - 1]^2$. Polloni *et al* have also shown that $P_\omega^{max} = P_\omega(T_{opt}) \equiv P_{2\omega}^{max}$, meaning that the maximum SH power from an ICSHG laser cannot exceed the optimal FH

#121572 - $15.00 USD Received 17 Dec 2009; revised 28 Jan 2010; accepted 29 Jan 2010; published 23 Feb 2010

power that can be extracted, under identical linear loss and pump parameter, from the laser equipped with an optimal output coupler.

Equation (2) was used to least-square fit the experimental data of Fig. 10b by taking as variable parameters y, P_{th}, and the multiplicative constant appearing in Eq. (2). The value of y leading to the lowest fit residual was found to be $y = 1.0 \equiv y_{opt}$ (and $P_{th} = 1.7$W, $I_{sat}(\pi w^2/2)L = 0.38$W), confirming that we have indeed achieved the ICSHG optimal coupling condition, a regime hardly emphasized on in most of the reported cw ICSHG experiments which rather focused on optical-to-optical efficiencies ($P_{2\omega}/P_{abs}$~10% at maximum here). The fit agreement with Eq. (2) indicates that thermal effects are negligible up to $P_{abs} = 15$W. Displayed in Fig. 10b is the red power (square symbols) obtained with a 10mm type-I-cut BiBO ($\theta = 8.6°$, $\varphi = 0°$) which, when fitted with Eq. (2), yields $y = 0.1$ far from optimal SHG coupling. Furthermore, the optimal condition $y_{opt} = 1$ is equivalent to the following equality,

$$\left(l_c \frac{w}{w_0}\right)^2 = \frac{\varepsilon_0 c L \lambda_\omega^2}{4\pi^2 (d_{eff}^2 / n^3) I_{sat} G} \tag{3}$$

relating the nonlinear crystal length to its figure-of-merit, to the focusing ratio w/w_0 and to the saturation intensity of the transition. Equation (3) is useful to evaluate the necessary crystal length or the ring resonator mode waist ratio to achieve $y = 1$. Using $d_{eff} = 9$pm/V, n(ppKTP)≈1.8, $L = 0.03$, $w/w_0 = 6.5$, $I_{sat} = 6.7$ kW/cm^2 and G≈0.92 [48] the calculated ppKTP length to achieve optimal coupling is l_c≈10.13mm, close to the experimental value used. Using a non-critically phase-matched BiBO ($d_{eff} = 3$pm/V, walkoff $\rho = 25$mrad), a ~3 × longer crystal would be necessary to achieve optimal ICSHG coupling. In Fig. 10b, the combined effect of spatial walkoff and low nonlinear figure-of-merit is responsible for the low $y = 0.1$ parameter found for BiBO.

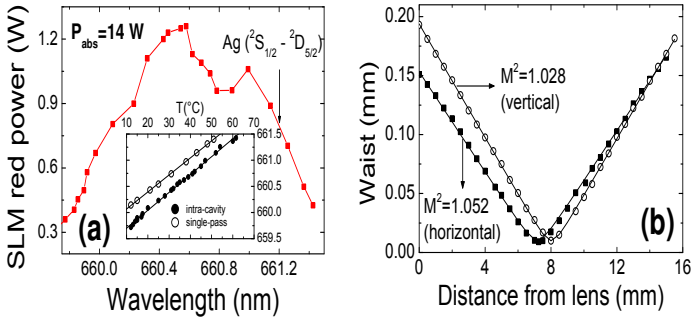

Fig. 11. (a) Red power (uncorrected for the transmission loss of M4) SLM tuning curve. The inset shows the red wave temperature tuning slope (+ 0.033nm/◦C) external (Fig. 2c) and internal to the cavity. (b) Red beam quality factors in the horizontal (squares) and vertical (circles) direction, showing a slight astigmatism.

Because the red laser is intended to perform high-resolution atomic spectroscopy, it is important to investigate the wavelength tuning behavior across the laser gain bandwidth. Red tuning over ~1.6nm (almost the full gain bandwidth) was achieved by etalon tilt (Fig. 11a), starting from the center-gain wavelength and using the adiabatic procedure described at the beginning of this section to avoid the partial KLM regime. The arrow in Fig. 11a indicates the position of the narrow two-photon resonance of atomic silver at 661.2nm, at which still 750mW of single-frequency power is available. The measured red beam quality factors (M^2~1.03, Fig. 11b) are those of a diffraction-limited beam (see Fig. 1b), which highlights the advantage of using a temperature-tuned ppKTP rather than a critically-phase-matched BiBO for which the red beam profile (M^2~1.3) was found quite elliptical due to spatial walkoff dephasing effect [8,9].

#121572 - $15.00 USD Received 17 Dec 2009; revised 28 Jan 2010; accepted 29 Jan 2010; published 23 Feb 2010

The inset of Fig. 11a plots (with solid circles) the final ppKTP temperatures derived from the tuning process, while the hollow circles are the quasi-plane-wave single-pass QPM temperatures measured in Section 3 (Fig. 2c). It is striking to note that the intracavity QPM temperatures are positively offset by + 8 to + 10°C, while the temperature tuning slopes are identical. Such a large offset cannot be explained by the temperature measurement uncertainties which do not exceed ± 2°C (the QPM acceptance bandwidth is ΔT = 10°C). It can neither be explained by the tight focusing effects which induce a negative QPM temperature shift as seen in Fig. 2c. One possible explanation that comes in mind may be that the oscillating mode at maximum red power is phase-mismatched ($\Delta k(\lambda_\omega,T)\neq 0$) with respect to the top of the QPM spectral curve. A first interpretation may then be that the residual nonlinear index of refraction $n_2 I_\omega$ imprinted to the FH wave may shift the optimum ppKTP temperature. We have checked this assumption by calculating the necessary amount (and sign) of nonlinear index required to cause a ΔT = + 5°C shift of the QPM temperature, substituting $n_e(\lambda_\omega,T)$ by $n_e(\lambda_\omega,T) + n_2 I_\omega$ in the $\Delta k(\lambda_\omega,T) = 0$ QPM condition. The result is that $n_2 I_\omega = + 3 \times 10^{-5}$ is required to produce such a positive shift which translates into a NLPS value of $\varphi_{NL} \sim (2\pi\, n_2 I_\omega l_c/\lambda_\omega) = + 1.42$ rad. From the measured single-pass SHG efficiency $P_{2\omega} = \Gamma_{SP} P_\omega^2$ ($\Gamma_{SP} = 3.8 \times 10^{-2}$ W/W^2 in Fig. 3c), an estimation of the intracavity FH power yields P_ω = 6W at maximum 1.4W red power. This FH power is much lower than the one (70W) used to plot the NLPS curve in Fig. 9a leading to a maximum φ_{NL} = 0.15 rad. Hence the assumption of a residual nonlinear index positively offsetting the QPM temperatures in Fig. 11 is not satisfactory. A more plausible explanation of this temperature shift may be due to the peculiar dynamics of the ICSHG laser under finite QPM bandwidth ($\gamma = \Delta\lambda_{NL}/\Delta\lambda_g < 1$) and large SH conversion conditions as studied theoretically and experimentally by Greenstein *et al* with a Nd:YAG/ppKTP laser [33,34]. In these works, they found that the gain-to-nonlinear loss competition among longitudinal modes may force the laser to oscillate on a longitudinal mode detuned on the left side (*i.e.* at $T > T_{QPM}$) of the single-pass QPM spectral acceptance curve corresponding to a temperature setting larger than for the actual oscillating mode (see Fig. 6 of Ref [34].). Equivalently, it is probable that the 10mm long ppKTP nonlinearity may already exceed the optimal-coupling condition: When experimentally maximizing the red output by playing on the temperature, the nonlinear laser reacts to this over-coupling by choosing a longitudinal mode substantially phase-mismatched with respect to the perfect QPM condition.

5. Summary and conclusions

In summary, we have demonstrated an optimally-coupled ICSHG Nd:YLF/ppKTP ring laser operating on the broad $^4F_{3/2}$-$^4I_{13/2}$ transition, capable of running in two different temporal regimes owing to the finite spectral bandwidth of the thick ppKTP crystal ($\gamma = \Delta\lambda_{NL}/\Delta\lambda_G < 1$). Without any spectrally selective intracavity etalon, the laser systematically undergoes a strong self-starting, self-pulsing dynamics at the cavity FSR frequency. This instability is attributed to partial but pure (cascaded) Kerr-lens mode-locking mechanism when the ppKTP is consequently temperature phase-mismatched, without any need for an intracavity hard aperture or for a nearly instable resonator condition as often required for KLM lasers. This is to our knowledge the first report of strong cascaded second-order KLM dynamics in a unidirectional ICSHG ring laser containing a Faraday optical diode and operating at the middle of its stability range. The mechanism leading to partial mode-synchronization, whichever the ppKTP temperature (leading to self focusing or defocusing), is different from CSM or NLM processes requiring a double-pass inside the nonlinear crystal, a condition relevant with standing-wave resonators. The strength of the observed dynamics and its insensitivity to critical cavity parameters as encountered in genuine $\chi^{(3)}$-based KLM lasers are attributed to the giant nonlinear phase-shift provided by $\chi^{(2)}$:$\chi^{(2)}$ cascading in ppKTP, and to the specific ring geometry used. These preliminary results should open the route to the realization of pure cascaded KLM Nd-ring lasers oscillating on the less investigated 1.3µm transitions, a spectral region for which the use of semi-conductor saturable absorber mode-lockers is problematic [38–40].

#121572 - $15.00 USD Received 17 Dec 2009; revised 28 Jan 2010; accepted 29 Jan 2010; published 23 Feb 2010

The transition from partial KLM to cw single-frequency tunable regime could be achieved only with the insertion of a suitably spectrally-selective etalon and a delicate interplay of various parameters, in order to quench the dominant dynamical regime. When cw SLM regime is achieved, the ICSHG laser could deliver a record 1.4W of diffraction-limited red single-frequency power at 661nm (10 fold increase with respect to the broadband pulsing output), reaching the theoretical limit of optimal SHG coupling predicted in the late 60's. Such ~100% conversion efficiency would have been difficult to achieve in an external cavity-enhanced SHG configuration. This cw tunable solid-state laser source is a convenient alternative to dye-lasers for high-resolution atomic spectroscopy in the red range.

Acknowledgments

This work is funded by the Laboratoire National de Métrologie et d'Essais (LNE/DRST, French National Bureau of Standards) within the frame of the joint laboratory LNE-Cnam (Conservatoire National des Arts et Métiers). F. A. Camargo acknowledges a PhD studentship grant from FAPESP (Brazil) and partial support from LNE/DRST. The authors are highly indebted to R. Kuselevitch (LPN-CNRS) and P. Georges (LCFIO-CNRS) for the temporary loan of their OSA and fast digital oscilloscopes, and to R. Sarrouf and T. Badr for marginal contributions to this work. The authors are also thankful to the anonymous referees for their valuable and constructive comments.

#121572 - $15.00 USD Received 17 Dec 2009; revised 28 Jan 2010; accepted 29 Jan 2010; published 23 Feb 2010